Holocene Climatic Changes in the Alaskan Arctic as Inferred from Oxygen-Isotopic Analysis

By

Richard S. Vachula

Thesis
for the
Degree of Bachelor of Science
in
Geology

College of Liberal Arts and Sciences
University of Illinois
Urbana-Champaign, Illinois

2015

Table of Contents

Abstract

Reconstructions of Holocene climate in the Alaskan Arctic allow for better understanding of how the region may respond to future climate changes. However, long-term records from the region are scarce. We conducted lithological and isotopic analyses at Wahoo Lake (69º 4.612, -146º 55.676) to infer Holocene climate variability in northern Alaska. Isotopic composition of modern water from this large, open-basin lake in the northern foothills of the Brooks Range suggests that winter precipitation dominates inputs to the lake. Isotopic composition of *Pisidium* exhibits large variations throughout the past 11,800 years, with $\delta^{18}O$ values ranging between 11.6 and 14.2‰ (VSMOW) and $\delta^{13}C$ between -2.3 and -7.1‰ (VPDB). Loss-on-ignition (LOI) shows high carbonate content (8.1-50.9%) in the subbasin sediments between 11.8-6.3 kcal BP, transitioning to lower carbonate (1.3-25.3%) and increased organic content (11.7-65.2%) between 6.3-1.4 kcal BP. High carbonate and elevated $\delta^{18}O$ values (13.0-14.0‰) from 11.5-8.5 kcal BP likely reflect lower lake level and possibly evaporative enrichment of lake water, suggesting warm, dry summers during the early Holocene. The disappearance of *Pisidium*, paired with a decrease in calcite deposition at ~6.5 kcal BP, suggests increasing lake-level in the mid-Holocene, which is supported by a basal date of 5.3 kcal BP from a core of the shallow shelf of the lake. This increase coincided with lake-level increases in interior Alaska and likely resulted from enhanced regional effective moisture. The shelf sediments exhibit a marked increase in carbonate content at ~3.5 kcal BP and $\delta^{18}O$ values generally rose from 12.4‰ at 3.5 kcal BP to 13.2‰ at 2.0 kcal BP (range = 11.6-14.2‰), suggesting increasing annual temperatures during this period. After 2.0 kcal BP, $\delta^{18}O$ values fluctuate between 11.9-13.3‰, but generally decline until 1.0 kcal BP, suggesting dramatic temperature fluctuations in the late Holocene. These Holocene variations in $\delta^{18}O$ values at Wahoo Lake generally correspond to

fluctuations in total solar irradiance, suggesting that solar variability may have played an important role in Holocene climate change of the Alaskan Arctic. Understanding the role of solar irradiance on natural variability of climate in this region provides a framework for evaluating climatic response and sensitivity to anthropogenic forcing.

Keywords

Arctic – *Pisidium* – Holocene – Solar Irradiance – Climate

Introduction

The amelioration of our understanding of Arctic climate history is important in light of the region's climatic sensitivity as well as its substantial warming since the mid-20th century (IPCC 2014). Holocene climate reconstructions help to create a historical context that can better inform our understanding of modern and future changes in this region. Paleoenvironmental proxies allow us to better understand natural climatic variability and associated forcing mechanisms. Pollen-based reconstructions have provided some insight into Holocene environmental changes in the Alaskan Arctic (Oswald et al. 1999, 2003, 2012, Anderson and Brubaker 1993, 1994, Mann et al. 2002, 2010). However, relying upon pollen records as climatological indicators is problematic because vegetation changes may occur in response ecological processes that are indirectly linked to climate. Thus, climate reconstructions based on non-pollen records are important to fully understand Holocene climatic history in the Alaskan Arctic.

Stable isotopes of carbonates can provide insight into past climate changes because the isotopic composition of a lacustrine carbonate is closely linked to the temperature of the water from which it formed as well as post-input modification processes such as evaporation (McCrea 1950, Epstein et al. 1953, Urey et al. 1951). The factors affecting isotopic composition in carbonates can be constrained by lithological indicators and an understanding of the modern constraints on the isotopic composition of the water from which the carbonates are precipitated, and thus carbonate isotopes are useful as paleoenvironmental indicators in lake sediments (Dansgaard 1964, Craig 1961, Fritz and Poplawski 1974, Bowen and Wilkinson 2002, Leng and Marshall 2004, Ito 2001, Leng et al. 2006). Carbonate isotope analyses of lake sediments have yielded important insight into the past climatic fluctuations. However, in Arctic regions, few sites have sufficient carbonate preservation to facilitate the use of isotopic variations for climatic reconstructions. In the Alaskan Arctic, only a small number of studies have used carbonate isotopes as paleoenvironmental indicators. Isotopic compositions of cellulose, chitin, and C*hara*-stem calcite encrustations have been utilized as proxies of environmental change in this region (Anderson et al. 2001, Clegg and Hu 2010, Wooller et al. 2012a). However there are no multi-decadal to centennial-scale resolution isotope records from the Alaskan North Slope, resulting in an incomplete understanding of Holocene climate in this region.

In this study, we examine lake sediments from a lake on Alaska's North Slope. Using the isotopic variations in fossil *Pisidium* as well as other sediment indicators of variations in lake hydrologic setting, we derive a high resolution paleolimnological isotope record of Holocene climate of the North Slope of Alaska. This new record offers a glimpse into the Holocene climatic history of this region and allows for a comparison with other regions of Alaska to better assess the large-scale atmospheric controls on climate change. Furthermore, we compare our record with variations in solar output to examine the relationship between solar forcing and climatic change in this region during the Holocene.

Study Sites

Wahoo Lake (69º 4.612 N, 146º 55.676 W, 707 m a.s.l.) is located in the Echooka River Valley in the northern foothills of the Brooks Range (Fig. 1A). Bedrock in the watershed consists of Permian and Triassic sandstone, siltstone, and shale of the Sadlerochit Group (Beikman 1980). Soils in the watershed are predominately gelisols underlain by permafrost, and vegetation is dominated by shrub-scrub tundra (NLDC 2006). Wahoo Lake is a large lake (0.28 km^2, 17.1 m maximum depth) with a large watershed (2.68 km^2), a single outlet, and two inlet streams (Fig. 1B). The bathymetry of this hydrologically open-basin lake is characterized by four subbasins, which are progressively deeper from east to west. Gastropod and bivalve shells were abundant along the shallow shelves and shoreline of the lake in the summer of CE 2011. Dissolved oxygen (DO) and temperature measurements from the water column at Wahoo Lake suggest that the lake was stratified in the summer of CE 2011, with a distinct epilimnion (0-3 m depth), metalimnion (3-5 m), and hypolimnion (5-8 m) (Fig 1C). The lack of DO in the hypolimnion suggests anoxic conditions at present.

The North Slope ecoregion experiences highly seasonal solar inputs resulting in below freezing air temperatures for about 9 months of the year and snow cover for more than 8 months of the year (Zhang et al. 1996, L'Heureux et al. 2004, Stone et al. 2002). Snowfall accounts for about 40% of total annual precipitation in the Arctic Foothills (Zhang et al. 1996). However, the sparse locations of weather stations paired with the use of gauges that may underestimate snowfall suggest that the contribution of winter precipitation may be much higher (L'Heureux et al. 2004, Zhang et al. 1996, Stafford et al. 2000). Spring snowmelt results in a rapid decrease in albedo from 75 to 17% within the span of several days, and the subsequent increase of solar absorption ushers in the short, albeit sunlight intense, summer growing season (Stone et al.

2002). Mean JJA (June-August) temperature and total JJA precipitation from the Toolik Lake weather station, approximately 120 km from Wahoo Lake, is 9.1 ºC and 193.1 mm, respectively (CE 1989-2014, 1988-2014 respectively, Environmental Data Center Team). Winter (December-February) mean temperature and precipitation are -22.1 ºC (CE 1989-2014) and 288.9 mm (CE 2009-2010, 2013-2014), respectively.

Methods

Modern Water Analysis

Temperature, dissolved oxygen concentration, and specific conductivity were measured using a YSI meter at 1-m increments in the water column of the eastern subbasin of Wahoo Lake. Water samples were obtained from inlet and outlet streams and at 1-m intervals in the water column of the lake using a Van Dorn sampler. Water samples were collected in 20 mL scintillation vials with conical caps that were sealed with electrical tape, and stored at 4 ºC in the laboratory prior to analysis. Samples were submitted to the University of Arizona and analyzed for $\delta^{18}O$ and δD using a Finnigan Delta S mass spectrometer and Finnigan /Device (precision <0.08‰ for $\delta^{18}O$ and <0.9‰ for δD).

Modern isotopic values of precipitation from the Barrow weather station were obtained from Global Network of Isotopes in Precipitation (GNIP) database (IAEA/WMO 2014) and used to construct a Regional Meteoric Water Line (RMWL; Fig 3). The Barrow GNIP isotopic data is representative of an irregular sampling of monthly precipitation from January 1962 to December 1969, as this was the only available dataset. Modeled monthly values of precipitation at Wahoo Lake were obtained from the Online Isotopes in Precipitation Calculator (OIPC; Bowen 2013, Bowen and Revenaugh 2003).

Sediment Analyses

Sediment cores were obtained from the eastern subbasin (8.1 m depth) and an adjacent shelf (2.8 m depth) in July 2011, using a modified Livingstone piston corer. To obtain the sediment-water interface at each site, we used a polycarbonate tube fitted with a piston, and the uppermost 20 and 30 cm of the shelf and subbasin cores, respectively, were extruded and subsampled in the field at 0.5-cm intervals. Overlapping cores segments from each site were split lengthwise and correlated using stratigraphic markers to assure a continuous sedimentary sequence from both coring sites. Loss-on-ignition (LOI) was performed on 0.5-cm^3 subsamples at continuous 1-cm resolution for the subbasin and shelf cores. Sample material was weighed after drying at 120 °C overnight and combustion at 550 °C for two hours and 950 °C for four hours in a muffle furnace. These measurements were used to calculate sediment bulk density (BD = g dry sediment cm^{-3}) and percentages of organic matter (OM% = % LOI at 550 °C), calcium carbonate ($CaCO_3$% = (% LOI at 950 ºC)*2.274), and residual lithic and ash (LA% = 100 – (OM% + $CaCO_3$%)).

Subsamples from both continuous cores were sieved through a 125-µm mesh with distilled water to isolate macrofossils for radiocarbon dating and carbonate analysis. *Pisidium* shells were isolated and prepared for isotopic analysis using a protocol adapted from Ito (2001). Briefly, shells were rinsed with deionized H_2O to remove sediment particles, transferred to a clean glass vial using 95% ethanol, immersed overnight in 2.5% NaOCl, triple rinsed with deionized H_2O, air dried, and ground to a fine powder with a mortar and pestle. Isotopic analyses were conducted at the Stable Isotope Laboratory of the Illinois State Geological Survey using a Kiel III carbonate device and Finnigan MAT252 isotope ratio mass spectrometer. Precision on laboratory standards is ±0.1 and ±0.15‰ for $\delta^{13}C$ and $\delta^{18}O$, respectively.

We measured ^{210}Pb activity on the uppermost sediments for both cores. Samples were prepared following the protocol of Eakins and Morrison (1978) and activity was measured with an Ortec OctêtePlus alpha spectrometer. The ^{210}Pb profile from the shelf sediments did not follow an exponential decay pattern, which may have been caused faulty spectrometer readings related to a black precipitate that formed on the planchettes. This issue precluded the use of ^{210}Pb dating for this core. The age for each sample depth for the subbasin core was obtained from ^{210}Pb activity using a constant rate of supply model (Oldfield et al. 1977, Binford 1990). For Accelerator Mass Spectrometry (AMS) ^{14}C dating, we followed the acid/base/acid procedure described in Oswald et al. 2005 to prepare ten terrestrial macrofossils, which were submitted to the Lawrence Livermore National Laboratory. Radiocarbon ages were calibrated to years before CE 1950 (cal BP) using the Intcal 09 dataset in Calib version 6.1.0 (Stuiver and Reimer 1993, Reimer et al. 2009). The ^{14}C ages (in addition to the ^{210}Pb ages for the subbasin core) were used to create 1,000 bootstrapped chronologies based on a weighted cubic smoothing spline function that was applied to the ages and their 2σ age range (Higuera et al. 2009). The resulting median ages and associated errors are used as the age-depth model for each core (Fig. 2).

Results

Modern Water

The temperature of the water column at Wahoo Lake ranged from 16.3 ºC at the surface to 3.5 ºC in the hypolimnion, with a well-defined thermocline between 4.0 and 5.0 m (Fig. 1C). Dissolved oxygen in the epilimnion (0-4.0 m) is 9.7 ppm, declining to 0.0 ppm in the bottom 3 m of the water column. The $\delta^{18}O$ values were generally lower from 0.0 to 5.0 m (-20.0 to -19.9‰), and higher from 6.0 to 7.0 m (-19.9 to -19.8‰).

The δD values from the Barrow weather station ranged from -18.2 to -223.3‰ and $\delta^{18}O$ values ranged from -4.2 to -29.0‰. The slope of the RMWL based on these data is 7.1243 $\delta D/\delta^{18}O$ (Fig. 3A inset). Online Isotopes in Precipitation (OIPC) values fall along the RMWL and have a very similar slope (7.097 $\delta D/\delta^{18}O$). The OIPC δD values range from -118 to -219‰ and $\delta^{18}O$ values range from -15.2 to -29.0‰. Inlet and outlet water isotopic values fall nearest the April, October, and February OIPC values. The outlet (δD = -162.0, $\delta^{18}O$ = -19.8) and surface water (δD = -162.5 and -162.9, $\delta^{18}O$ = -20.0 and -20.1) values are greater than those of the inlet streams (δD = -164.5 and -165.4, $\delta^{18}O$ = -20.8 and -21.1). Enrichment in ^{18}O and deuterium occurs between the inlets and the outlet, suggesting evaporation. However, the difference in values between these points falls within the variability of both the OIPC and Barrow station values; thus evaporation likely has limited effect on lake water composition.

Chronology

The age model of the Wahoo subbasin core spans from -0.06 to 11.9 kcal BP (Fig. 2) and all ^{14}C and ^{210}Pb ages are in stratigraphic order. The sediment accumulation rate is relatively stable around ~0.02 cm yr^{-1} in both cores, except for a period of rapid deposition (maximum of 0.2891 cm yr-1) in the subbasin core between 0.8 and 1.6 kcal BP. The shelf sediment core spans -0.06 to 5.3 kcal BP. The ^{14}C ages are in stratigraphic order and the sediment accumulation rate ranges from 0.0199 to 0.3403 cm yr^{-1}, with peak values between 2.0 kcal BP and 3.8 kcal BP.

Core Lithology

The basal sediments of the subbasin core are thinly (<10 cm) interbedded fine silts and clays with abundant *Pisidium* shells, $CaCO_3$% ranging from 8.1-50.9% (mean = 28.0%), and percentage of organic matter (OM%) from 3.7-38.0% (mean = 15.3%) (Fig. 4A). At 162 cm (6.3 kcal BP), the sediments transition to black gyttja with low $CaCO_3$% and high OM%. *Pisidium* shells are not present in this sedimentary unit. At 96 cm (1.4 kcal BP) the sediments transition to silt-rich gyttja. The $CaCO_3$% increases to 1.4-53.5% although *Pisidium* shells are rare. Residual lithic and ash (LA%) in the subbasin core (ranging from 28.5 to 75.2%) is greater in the basal sediments and lower following the gyttja transition.

The basal sediments of the shelf core contain abundant moss fragments, with OM% ranging from 39.6-79.3% (mean = 55.9%), LA% from 9.08-57.11% (mean = 38.3%), and $CaCO_3$% from 1.2-13.5% (mean = 5.8%) (Fig. 4B). At 200.5 cm (3.5 kcal BP) sediments transition to thinly laminated fossiliferous gyttya with $CaCO_3$% ranging from 24.8-74.2% (mean = 49.0%), OM% from 12.5-50.1% (mean = 28.6%), and LA% from 1.10-49.94%, (mean = 22.3%). At 34 cm (0.9 kcal BP), there is a change from *Pisidium* to gastropod fauna. These gastropod shells proved unreliable as isotopic indicators after preliminary investigation.

Carbonate Isotopes

Isotopic compositions of *Pisidium* shells throughout the past 11,800 years exhibit large variations, with $\delta^{18}O$ values ranging between 11.6 and 14.2‰ (VSMOW) and $\delta^{13}C$ ranging between -2.3 and -7.1‰ (VPDB) (Fig. 4C). The lack of carbonate preservation in the subbasin core between 7.2-3.5 kcal BP results in a mid-Holocene gap in the isotopic record. From 11.8 to 9.0 kcal BP, $\delta^{18}O$ values are relatively high (12.9-14.0‰) and are followed by a marked decrease to 12.4‰ at 7.3 kcal BP and a subsequent increase to 12.4‰ at 7.1 kcal BP. The $\delta^{13}C$ values in the early Holocene vary between -6.5 to -4.6‰ and generally decline through time.

Late-Holocene isotopic data are from *Pisidium* preserved in the shelf core (with the exception of one subbasin isotopic value at 1.4 kcal BP). From 3.5 to 0.9 kcal BP, $\delta^{18}O$ and $\delta^{13}C$ values exhibit high frequency fluctuations (11.6 to 14.2‰ and -2.3 to 7.1‰, respectively). From 3.5 to 2.0 kcal BP, $\delta^{18}O$ generally increases from 12.4‰ to 13.2‰, although variability is high. Values subsequently decline overall to a minimum (11.6‰) at 1.8 kcal BP. From 1.8 to 1.5 kcal BP $\delta^{18}O$ increases to 13.3‰, and then declines to 12.6‰ at 1.1 kcal BP. This decline is followed by an increase to 13.1 ‰ at 0.9 kcal BP. From 3.5 to 2.8 kcal BP, $\delta^{13}C$ decreased from -7.1 to -3.4‰ after which there was an increasing trend until 2.0 kcal BP (ranging from -7.1 to -2.3‰). From 2.0 to 0.9 kcal BP, $\delta^{13}C$ values decreased (ranging from -2.3 to -5.8‰). The $\delta^{18}O$ and $\delta^{13}C$ values of the *Pisidium* are not correlated (R= 0.13, p-value = 0.24). However, the two records share broadly similar trends on multi-millennial timescales, with the general pattern of decreasing values from 11.8-7.2 and 2.0-0.9 kcal BP, and increasing values from 3.5-2.0 kcal BP in both records.

Discussion

Controls on carbonate isotopic composition

Two factors control the isotopic composition of *Pisidium*: the isotopic composition of the water from which the carbonate is precipitated, and the temperature at which carbonate formation occurs. The influence of temperature on *Pisidium* shell isotopic composition is about 0.24‰ $^{o}C^{-1}$, assuming equilibrium conditions, which is small compared to the factors that can result in large differences in the isotopic composition of water (Craig 1965). For example, the temperature at which meteoric precipitation occurs can alter the isotopic composition of water by about 0.2 to 0.7 ‰ $^{o}C^{-1}$ (Dansgaard 1964). Evaporative enrichment alters the composition of water by several per mille, with the magnitude depending upon the humidity and temperature of the atmosphere under which it occurs (Dansgaard 1964). Comparably, the relative seasonality of the meteoric precipitation contributing to the lake water budget can result in several per mille deviations in the lake water isotopic composition. Thus, it is unlikely changes in water temperature alone resulted in the large $\delta^{18}O$ variations at Wahoo Lake.

The Wahoo lake water is relatively depleted in ^{18}O and ^{2}H compared to precipitation at the Barrow weather station. This depletion is likely the result of inland movement of moisture from Barrow weather station, which is 445 km from Wahoo. Lake water isotopic measurements from Wahoo Lake plot near modelled winter and spring OIPC (Online Isotopes in Precipitation Calculator) precipitation values (Fig. 3A). This indicates that the modern water budget of Wahoo Lake is dominated by winter precipitation, a pattern that has been documented at lakes from the southern Brooks Range (Clegg et al. 2010). Spring snowmelt occurs when the ground is still frozen, and thus meltwater reaches lakes via overland flow and ephemeral streams. The inlet water isotopic values from Wahoo Lake are the most depleted in ^{18}O and deuterium, which reinforces this interpretation that input water to the lake largely derives from snowmelt, even in the summer months. In comparison, summer precipitation is more likely to be absorbed by plants and soils in the watershed and thus contributes less overall to the lake water isotopic signal.

Evaporation of water in lakes with a long residence time can result in post-input isotopic fractionation. Wahoo Lake is hydrologically open at present, although the residence time of water may be high due the large area and depth of the lake. The difference in the inlet versus outlet and lake water isotopic values of Wahoo Lake indicates that water becomes more enriched in ^{18}O during its residence in the lake basin. However, the isotopic difference between inlet and outlet stream water is small (~1‰), and so the influence of evaporation on Wahoo lake water isotopic composition is likely limited. Additionally, the isotopic composition of the modern water samples fall within the variability of the isotopic composition of precipitation from the GNIP (Global Network of Isotopes in Precipitation) station data and OIPC modelled values from the lake (Fig. 3B). Furthermore, if evaporation affected the isotopic composition of the epilimnion, then we would expect enrichment of ^{18}O in the surface waters compared to the hypolimnion. However, the $\delta^{18}O$ of epilimnion water column samples are depleted in ^{18}O relative to deeper waters (Fig. 1C), suggesting a limited influence of evaporation at Wahoo Lake at present.

Hydrologic setting can influence the relative controls on the isotopic of lake water, with small, closed-basin lakes being highly influenced by evaporative enrichment compared to large, open-basin settings which are more sensitive to temperature and seasonality of precipitation (Leng and Marshall 2004). The lithologic changes in the Wahoo Lake sediment cores allow insight into the hydrologic setting and provide a framework for interpreting the variations in carbonate $\delta^{18}O$ through time. From 11.8 to ca. 6.0 kcal BP, the fine grained subbasin sediments with high lithic content (Fig. 4A) suggests high allocthonous inputs in a relatively low energy setting. Additionally, high $CaCO_3$% and the presence of *Pisidium* shells indicate high carbonate production, which requires a high concentration of Ca^{2+} ions. These data suggest that Wahoo Lake may have been a shallow and well-mixed basin in the early Holocene, and thus we interpret out isotopic record in this hydrological context. The isotopic values of *Pisidium* were likely influenced by evaporative enrichment in this closed basin setting and are thus useful as a proxy for changes in effective moisture in the early Holocene. The lithological change to black gyttja with higher OM% and low $CaCO_3$% at ca.6.5 kcal BP (Fig. 4A) suggest that lake level rose during the mid-Holocene and resulted in a stratified lake setting. Increased lake-level also explains the decrease in $CaCO_3$% and the disappearance of *Pisidium* shells in the subbasin core, as increasing lake level likely resulted in a change to open-basin conditions that could have interrupted evaporative concentration and precipitation of carbonate. The basal date of the shelf core is 5.3 kcal BP (Fig. 4B), suggesting that lake levels continued to rise and resulted in sediment deposition on the shelf by this time. The sediments of the shelf core do not show any indication of a sedimentary hiatus and we assume that the lake level remained high and that the basin was hydrologically open from the middle Holocene to present. Modern water isotopic measurements suggest limited influence of evaporative enrichment on isotopic values. Therefore, we interpret variations in *Pisidium* $\delta^{18}O$ values during the late Holocene as proxy indicators of annual temperature variations and/or variations in the seasonality of annual precipitation.

Holocene climate variability

This carbonate isotope record from Wahoo Lake is one of the first for the North Slope, adding to a growing body of paleoclimatic reconstructions of Alaska during the Holocene. Models of Beringian climate suggest that the North Slope region was likely warm and dry during the Holocene Thermal Maximum (HTM; 11.5-9.0 kcal BP) (Bartlein et al 1992). Warming associated with the HTM has been identified in a number of paleorecords throughout the Arctic, although the influence of the HTM is not ubiquitous (Kaufman et al 2004, Kaufman et al. in press). The $\delta^{18}O$ record from Wahoo Lake shows relatively high values (12.9-14.0‰) in the early Holocene (12.0 to 9.0 kcal BP) (Fig. 4C), suggesting high evaporative enrichment during the HTM. Other records from the Alaskan Arctic indicate that this period was generally warm and dry. For example, lake level studies from interior and northern Alaska indicate that the early Holocene was characterized by low lake levels, possibly facilitated by warm and dry summer conditions (Abbott et al. 2000, Barber and Finney 2000, Finkenbinder et al. 2014, Gaglioti et al. 2014, Edwards et al. 2000). Consistent with this interpretation, analysis of trace elements in ostracods from a lake in the Alaska Range suggests that Holocene summer temperatures increased during this period (Hu et al. 1998). The thaw of ice wedges, increased permafrost active layer detachment and alluvial valley aggradation, and the proliferation of thaw lakes on the Seward Peninsula (Hopkins et al. 1960, Mann et al. 2010, Anthony et al. 2014) further suggest high summer temperatures in the early Holocene. The $\delta^{18}O$ values of *Pisidium* at Wahoo Lake decreased from 9.0 to 7.3 kcal BP, suggesting an increase in effective moisture following this arid interval. This pattern is consistent with pollen records from the North Slope that suggest increased biomass 11.3- 10.0 kcal BP was facilitated by warm, dry soils and the expansion of *Betula*, with a subsequent increase in effective moisture from 10.0-7.5 kcal BP (Oswald et al. 2003, 2012).

The lack of *Pisidium* preservation precludes a detailed reconstruction of climatic conditions in the middle Holocene. The $\delta^{18}O$ values from 7.3 to 7.2 cal BP indicate a short interval of enhanced aridity prior to the hiatus in *Pisidium* shell preservation. The sedimentary change to black gyttja with high OM content and lack of carbonates suggest that the lake level at Wahoo Lake increased, with summer stratification resulting in an anoxic hypolimnion. Similar increases in mid-Holocene lake levels have been identified in several records from northern and interior Alaska (Mann et al. 2002, Edwards et al. 2000, Bigelow 1997, Finney et al. 2012, Abbott et al. 2000, Barber and Finney 2000, Finkenbinder et al. 2014). Enhanced moisture from 8.0 to 5.0 kcal BP has been well documented in Brooks Range isotope and pollen studies (Clegg and Hu 2010, Oswald et al. 2003, 2012, Anderson et al. 2001). This moisture increase has been attributed to increased prevalence of a westerly Aleutian Low, which enhanced moisture delivery to the Alaskan interior (Chipman et al. 2012, Rodionov et al. 2007). Evidence of glacial advances in the Brooks Range at 5.0 kcal BP also indicates high moisture and cooler summer temperatures during the middle Holocene (Ellis and Calkin 1984). The Wahoo Lake record, in the context of these regional trends, suggests that the middle Holocene increase in effective moisture was widespread throughout Alaska.

At ca. 3.5 kcal BP, CaCO3% increased and *Pisidium* shell preservation recommenced in the shelf core. Carbonate shells were abundant throughout the past 3,500 years in the shelf core, although no *Pisidium* shells were present after 0.9 kcal BP. Shallow water on the shelf with ample light penetration likely provided a habitat for *Pisidium* growth as well as minimal carbonate dissolution. The high frequency $\delta^{18}O$ variations (ranging from 11.6 to 14.2%) from 3.5 to 0.9 kcal BP suggest that the late Holocene was characterized by marked fluctuations in temperature or seasonality of precipitation. An abrupt increase in temperature at 4.0 kcal BP, noted in a reconstruction of average temperatures derived from chlorophyll abundances in nearby Kurupa Lake (Fig. 1A), may have facilitated the return of *Pisidium* (Boldt et al. 2015). High $\delta^{18}O$ values could result from warmer temperatures during precipitation or a shift to increased proportion of water from summer precipitation inputs. These large temperature fluctuations in the late Holocene, suggested by the large variations in our *Pisidium* $\delta^{18}O$ record, coincide with records of glacial advance throughout Alaska. Prominent troughs in $\delta^{18}O$ values of our record suggest periods of decreased temperature centered at or ranging from 1.1, 1.8, 2.2, 2.5, 2.7-2.8, 2.9-3.1, and 3.3-3.4 kcal BP (Fig. 4C). Glacial advances were noted from 3.3 to 2.9 kcal BP in the Alaska Range, the Wrangell-St. Elias mountains, and the Kenai Mountains (Young et al. 2009, Barclay et al. 2009a,b). Additionally, in the Brooks Range, lichen and ^{10}Be derived moraine ages of 3.3, 2.7, 2.6, and 2.5 kcal BP indicate glacial advances (Ellis and Calkin 1984, Solomina and Calkin 2003, Badding et al. 2013, Evison et al. 1996). A second period of Alaskan glacial advance is identified in the Wrangell Mountains at 2.0 kcal BP and in the Coast Mountains from 2.2 to 2.0 kcal BP (Wiles et al. 2002, Rothlisberger 1986). In a recent review, Solomina et al. identified three periods of Alaskan mountain glacier expansion; 4.5-4.0, 3.3-2.9, and 2.2-2.0 kcal BP (Solomina et al. 2015).These periods of widespread glacial advance from ca. 3.3 to 2.0 kcal BP largely coincide with our record of low temperatures, with our greatest $\delta^{18}O$ values (highest temperatures) coinciding with the transitional periods between advances. This indicates a link between Alaskan glacial activity and North Slope climate. The late-Holocene consistency of our isotopically derived North Slope climatic record and Alaska-wide glacial advancement records, suggests that North Slope temperature regimes and Alaskan glacial dynamics may respond to the same forcing factors. Solomina et al. 2015 found a coincidence of global Neoglacial advances with multi-decadal periods of low solar activity, suggesting that during the late Holocene, variability of solar ablation was likely a primary forcing of glacial advance and retreat. The relationship between our record and records of Alaskan glacial activity thus suggests that high latitude and high altitude sites may have been similar in their sensitivity to solar variability.

Solar irradiance and climate in the Arctic

Natural solar output variability is an important component of the complex feedback mechanisms in the Arctic. Solar irradiance has been linked to Arctic climatic variability during the Holocene (Hu et al. 2003, Anchukaitis et al. 2013, Clegg et al. 2011), but such linkages remain controversial. Steinhilber at al. (2012) produced a Holocene record of total solar irradiance (TSI) derived from ^{10}Be in Antarctic and Greenland ice cores as well as ^{14}C in tree rings (Fig. 5). The variations in this TSI record correspond broadly to variations in our $\delta^{18}O$ record from Wahoo Lake (Fig. 5A). In general, both records exhibit high TSI and $\delta^{18}O$ values from 1.1 to 1.6, 1.8 to 2.5, 3.0 to 3.3, 7.1 to 7.3, and 8.9 to 9.3 kcal BP, and low from 0.9 to 1.4, 2.5 to 3.2, and 7.2 to 8.8 kcal BP. A 9-pt smoothing of TSI (22 year resolution) and 11-pt smoothing of $\delta^{18}O$ (~30 year resolution) share a significant, weak correlation (R = 0.28, p-value = 0.037). The relationship between our $\delta^{18}O$ record and TSI variability suggest that variations in solar output may have been an important driver of North Slope climate changes on multi-decadal timescales.

The OM% and $\delta^{13}C$ also co-vary with changes in the TSI record (Fig. 5B, C). These three records exhibit periods of high values 1.5-5.5 and 8.6-9.2 kcal BP, as well as low values from 1.2-1.4 and 6.0-9.4 kcal BP. Linear regression analysis reveals that resampled, detrended TSI shares significant relationships with detrended OM% and $\delta^{13}C$. A 3-pt smoothing of TSI and $\delta^{13}C$ share a significant, weak correlation (R = 0.29, p-value = 0.022). A 3-pt smoothing of OM% and TSI share a significant, moderate correlation (R = 0.48, p-value = 2.49 E-11). Multiple factors can affect the $\delta^{13}C$ value of lake water, including; atmospheric exchange with CO_2, changes in watershed vegetation, photosynthesis, and respiration (Leng and Marshall 2004). While we cannot determine the precise mechanism that controlled the $\delta^{13}C$ fluctuations at Wahoo Lake, the general consistency between $\delta^{13}C$ and OM% suggests that these metrics are related to changes in lake productivity. Increased freshwater productivity in the Arctic has been linked to periods of higher temperatures, increased permafrost thaw, and longer ice-free seasons (Prowse et al. 2006). Thus downcore changes in OM% and $\delta^{13}C$ values may thus be indicative of changes in productivity resulting from the indirect effects of solar variability. For example, increased TSI can result in earlier spring snowmelt, which can enhance climate warming via albedo feedbacks, as well as directly influence lake productivity by increasing the length of the growing season (Chapin et al. 2005, Stone et al. 2002).

Our lake-sediment record suggests that climate in the Wahoo Lake area likely responded to changes in TSI throughout the Holocene, which has important implications in light of recent anthropogenic forcing of climate change. Other studies have identified similar responses to sub-orbital scale TSI variability (Bond et al. 2001, Fleitman et al. 2003, Gupta et al. 2003, Hodell et al. 2001, Hu et al. 2003, Anuchukaitis et al. 2013, Clegg et al. 2011); however our understanding of the climatic and ecological response to these natural variations remains fragmented and controversial. Variability in the Asian southwest monsoon (Gupta et al. 2003), regime changes in the Indian monsoon (Fleitman et al. 2003), and Central American drought frequency (Hodell et al. 2001) have all been tied to natural variability in solar output. Additionally, climatic changes in high-latitude regions such as the North Atlantic (Bond et al. 2001), North American sub-polar regions (Hu et al. 2003, Anuchukaitis et al. 2013, Clegg et al. 2011), and the Arctic (Soon et al. 2005) have been tied to sub-orbital solar output cyclicity. Our understanding of the natural variability of Arctic climate is of paramount importance if we are to fully anticipate how increasing concentrations of atmospheric greenhouse gases coupled with variations in solar irradiance will affect the stability of the climate system in the future.

Figures

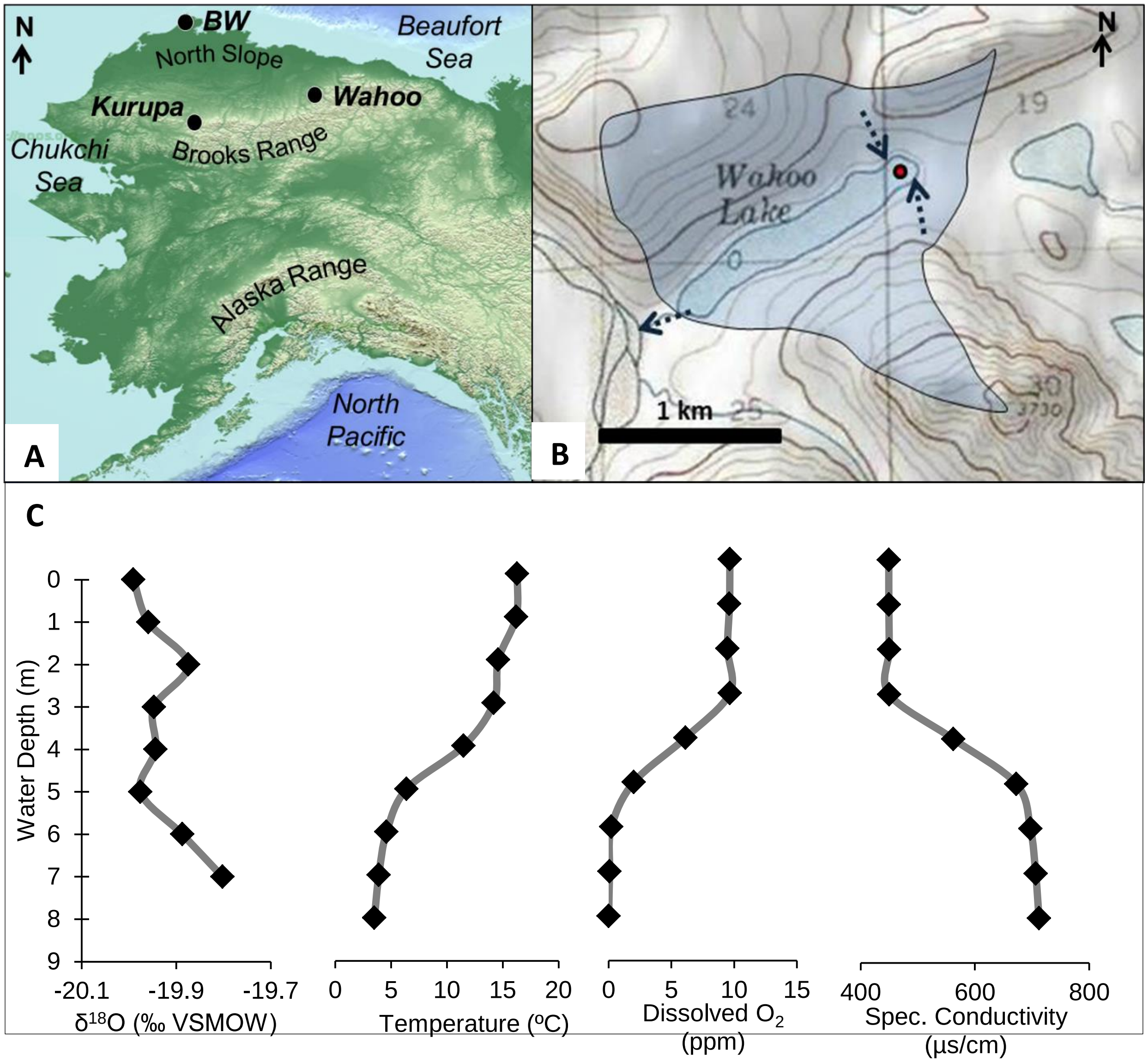

Figure 1: A) Map of Alaska with Barrow weather station (BW), Wahoo Lake, and Kurupa Lake marked with black dots. B) Watershed (shaded blue) delineation of Wahoo Lake, with red dot marking approximate coring site and dashed arrows indicating inlets and outlet. C) Modern water column measurements from Wahoo Lake.

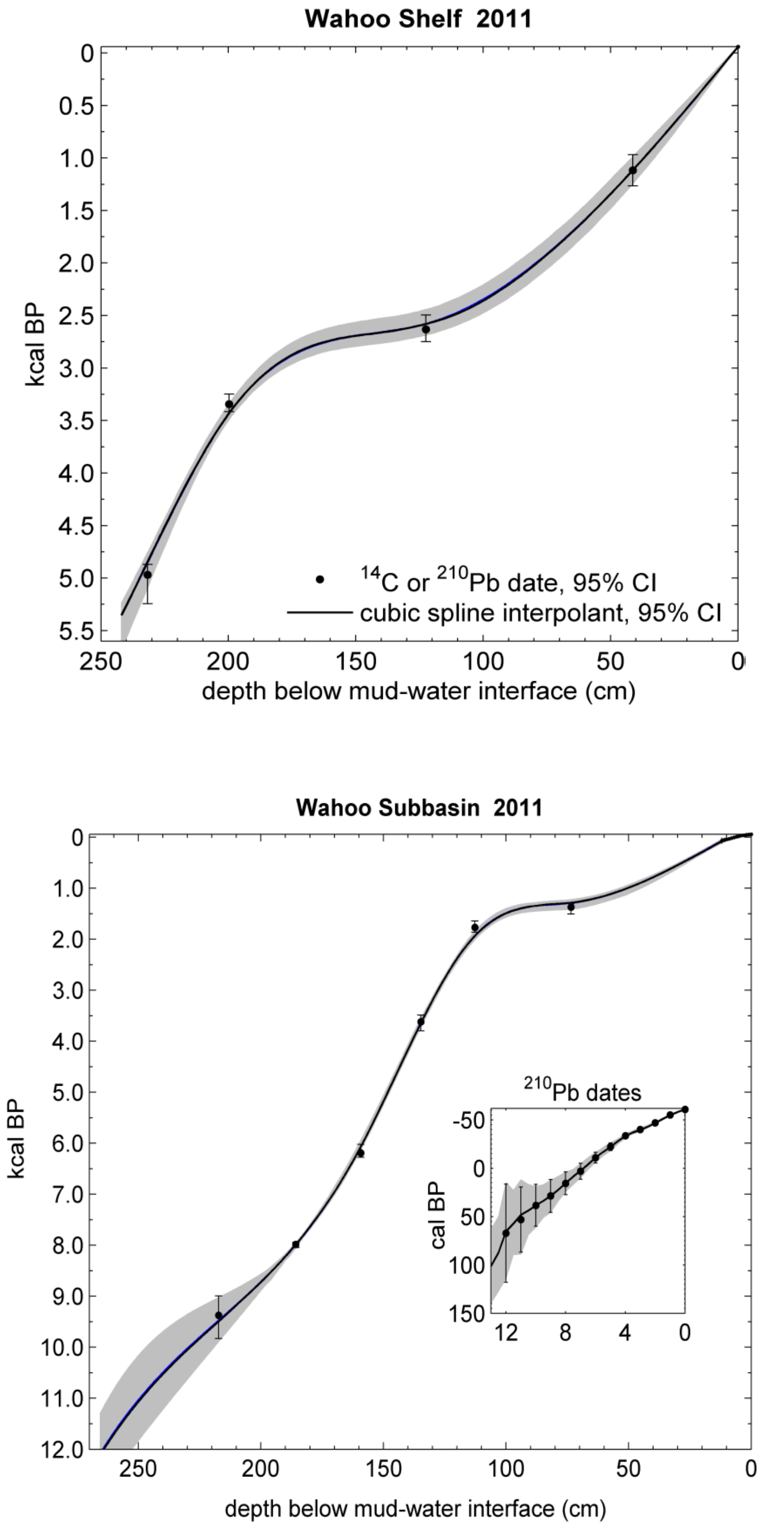

Figure 2: Depth-age models of Wahoo shelf and subbasin cores.

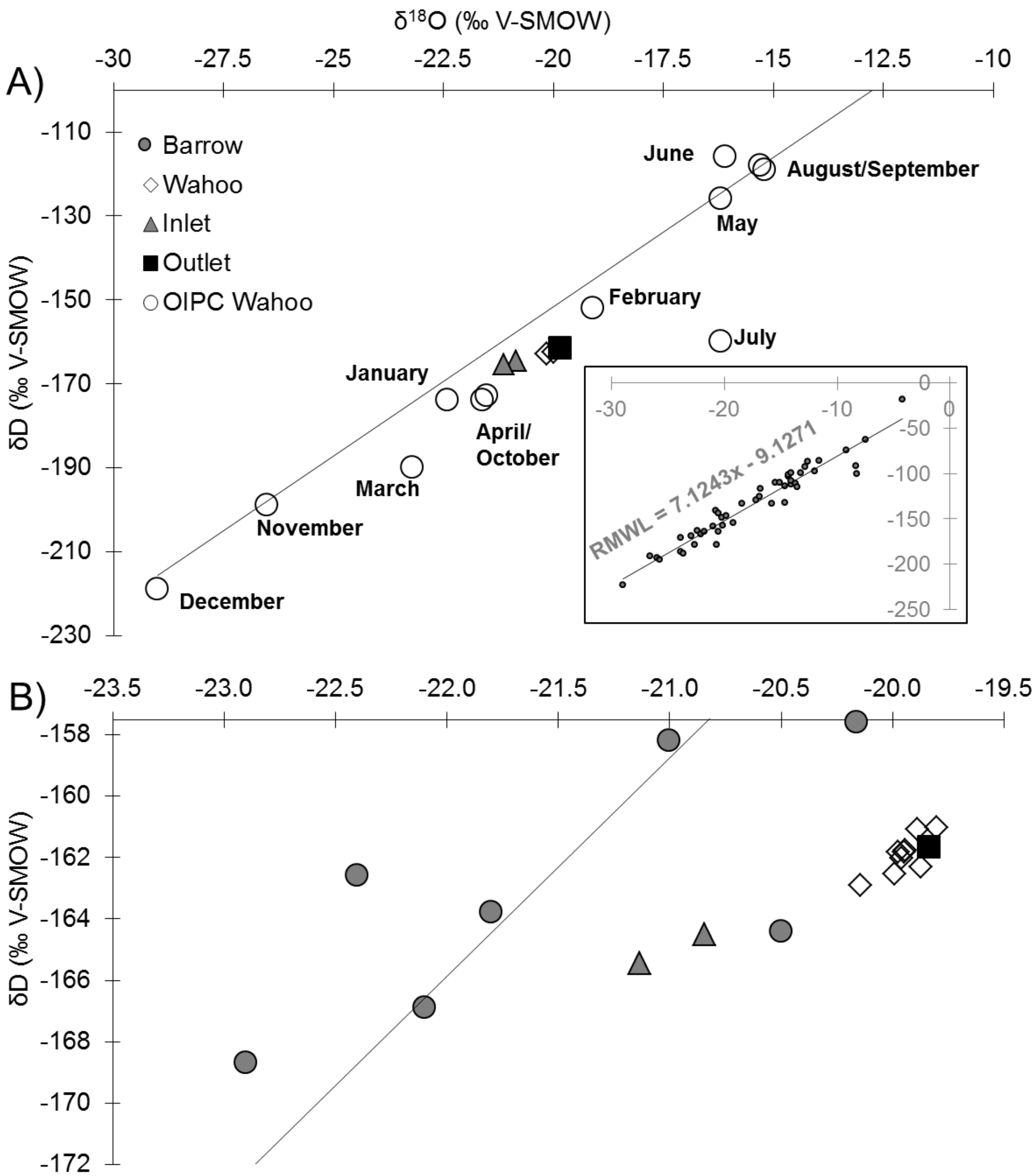

Figure 3: A) Modern Isotope samples with OIPC modelled seasonal precipitation values (open circles) for Wahoo Lake plotted with RMWL. Inlet samples denoted as gray triangles, outlet values as black squares, and lake water values as open diamonds. Inset: Barrow GNIP data (gray circles outlined black) used to construct RMWL. B) Water-column and inlet/outlet isotopic samples from Wahoo Lake plotted with the RMWL.

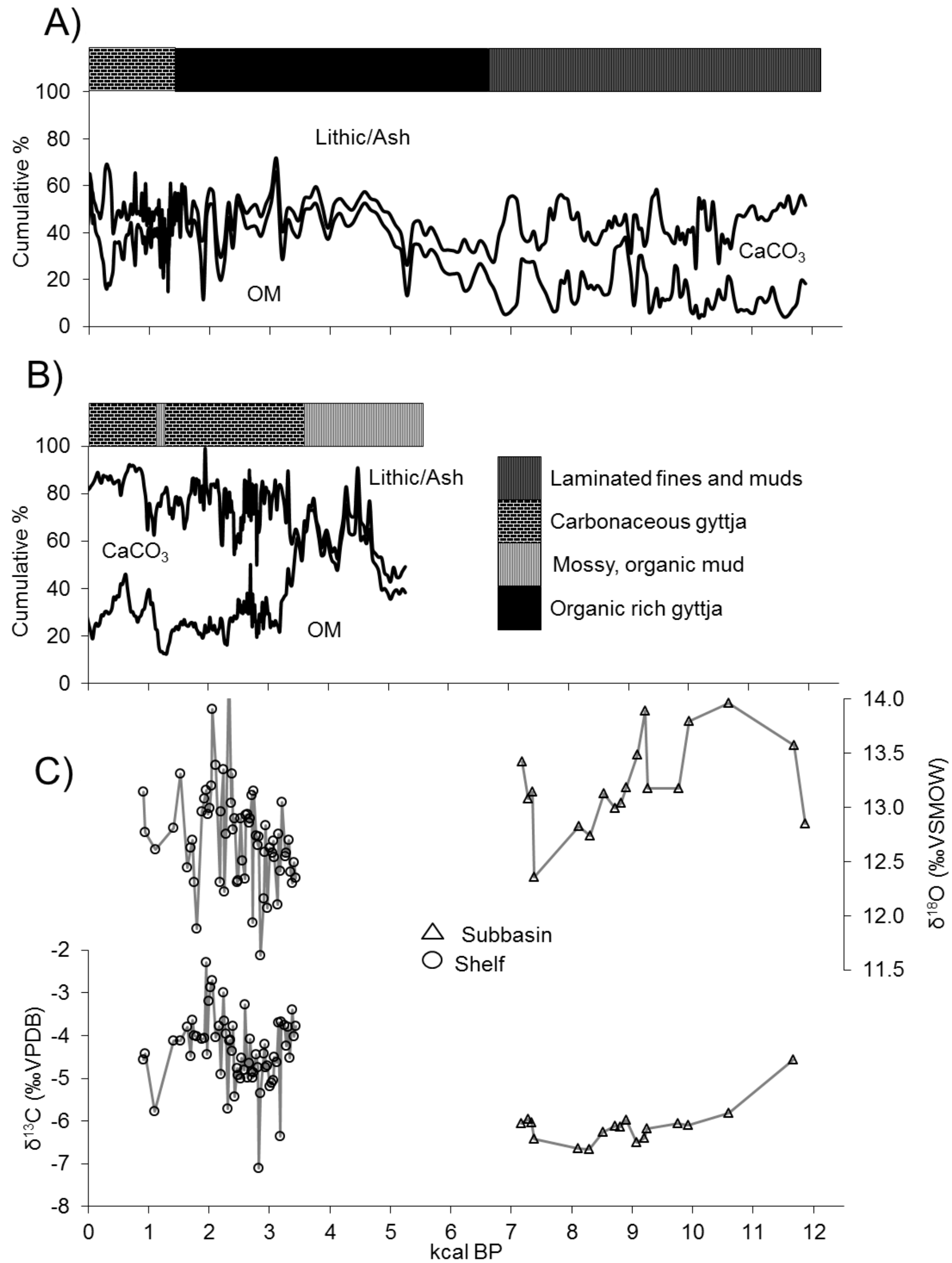

Figure 4: A) General core lithology, LOI derived sediment composition of the subbasin core. B) Same for shelf core. C) *Pisidium* $\delta^{18}O$ (top) and $\delta^{13}C$ (bottom) record, with open circles showing shelf points and triangles showing subbasin points.

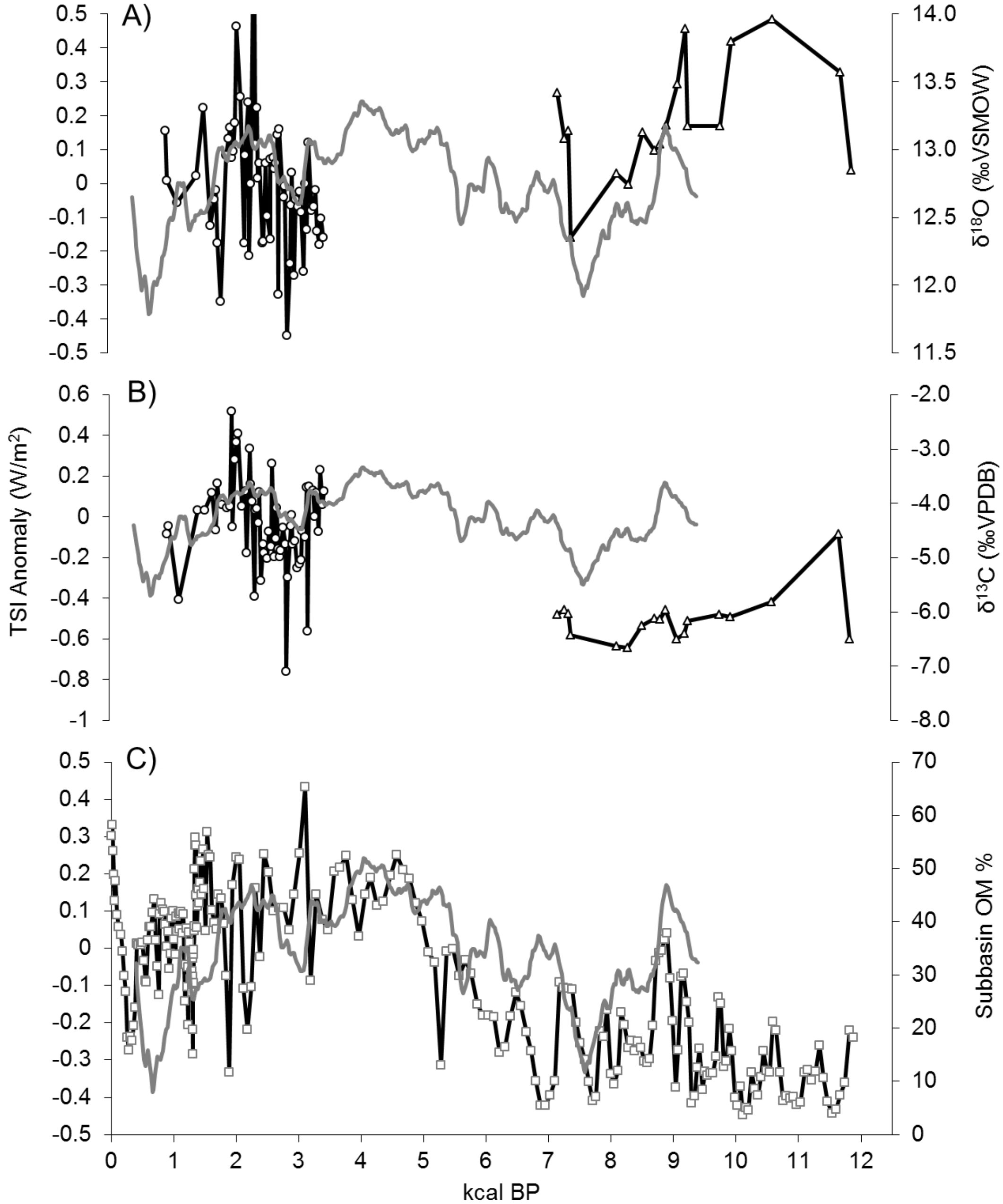

Figure 5: A) *Pisidium* δ^{18}O record, with open circles showing shelf points and triangles showing subbasin points, with Record of Holocene Total Solar Irradiance (TSI) anomalies derived from radiogenic nuclide ^{10}Be in ice cores, plotted with 20-point moving average (Steinhilber et al. 2009) in gray. B) *Pisidium* δ^{13}C record, same notation and TSI curve as panel A. C) LOI-derived organic matter (OM%) variation in subbasin core with TSI in gray.

References

Abbott, M. B., Finney, B. P., Edwards, M. E., & Kelts, K. R. (2000). Lake-level reconstruction and paleohydrology of Birch Lake, central Alaska, based on seismic reflection profiles and core transects. Quaternary Research, 53(2), 154-166.

Anchukaitis, K. J., D'Arrigo, R. D., Andreu-Hayles, L., Frank, D., Verstege, A., Curtis, A., ... & Cook, E. R. (2013). Tree-Ring-Reconstructed Summer Temperatures from Northwestern North America during the Last Nine Centuries*. *Journal of Climate*, *26*(10), 3001-3012.

Anderson, L., Abbott, M. B., & Finney, B. P. (2001). Holocene climate inferred from oxygen isotope ratios in lake sediments, central Brooks Range, Alaska. Quaternary Research, 55(3), 313-321.

Anderson, P. M., & Brubaker, L. B. (1993). Holocene vegetation and climate histories of Alaska. *Global climates since the last glacial maximum*, 385-400.

Anderson, P. M., & Brubaker, L. B. (1994). Vegetation history of northcentral Alaska: a mapped summary of late-Quaternary pollen data. *Quaternary Science Reviews*, *13*(1), 71-92.

Anthony, K. W., Zimov, S. A., Grosse, G., Jones, M. C., Anthony, P. M., Chapin III, F. S., ... & Frolking, S. (2014). A shift of thermokarst lakes from carbon sources to sinks during the Holocene epoch. *Nature*.

Badding, M. E., Briner, J. P., & Kaufman, D. S. (2013). 10Be ages of late Pleistocene deglaciation and Neoglaciation in the north-central Brooks Range, Arctic Alaska. *Journal of Quaternary Science*, *28*(1), 95-102.

Barber, V. A., & Finney, B. P. (2000). Late Quaternary paleoclimatic reconstructions for interior Alaska based on paleolake-level data and hydrologic models. *Journal of Paleolimnology*, *24*(1), 29-41.

Barclay, D. J., Wiles, G. C., & Calkin, P. E. (2009). Holocene glacier fluctuations in Alaska. Quaternary Science Reviews, 28(21), 2034-2048.

Barclay, D. J., Wiles, G. C., & Calkin, P. E. (2009). Tree-ring crossdates for a First Millennium AD advance of Tebenkof Glacier, southern Alaska. Quaternary Research, 71(1), 22-26.

Bartlein, P. J., Anderson, P. M., Edwards, M. E., & McDowell, P. F. (1991). A framework for interpreting paleoclimatic variations in eastern Beringia. Quaternary International, 10, 73-83.

Beikman, H. M. (1980). Geological map of Alaska. *US Geological Survey Map, scale*, *1*(2,500,000).

Bigelow, N. H. (1997). *Late-Quaternary Climate and Vegetation in Interior Alaska* (Doctoral dissertation, PhD Dissertation, University of Alaska, Fairbanks).

Binford, M. W. (1990). Calculation and uncertainty analysis of 210Pb dates for PIRLA project lake sediment cores. Journal of Paleolimnology, 3(3), 253-267.

Boldt, B. R., Kaufman, D. S., McKay, N. P., & Briner, J. P. (2015). Holocene summer temperature reconstruction from sedimentary chlorophyll content, with treatment of age uncertainties, Kurupa Lake, Arctic Alaska. The Holocene, 0959683614565929.

Bond, G., Kromer, B., Beer, J., Muscheler, R., Evans, M. N., Showers, W., ... & Bonani, G. (2001). Persistent solar influence on North Atlantic climate during the Holocene. *Science*, *294*(5549), 2130-2136.

Bowen, G. J. (2013) The Online Isotopes in Precipitation Calculator, version 2.2. http://www.waterisotopes.org.

Bowen, G. J., & Revenaugh, J. (2003). Interpolating the isotopic composition of modern meteoric precipitation. *Water Resources Research*, *39*(10).

Bowen, G. J., & Wilkinson, B. (2002). Spatial distribution of δ18O in meteoric precipitation. Geology, 30(4), 315-318.

Chapin, F. S., Sturm, M., Serreze, M. C., McFadden, J. P., Key, J. R., Lloyd, A. H., ... & Welker, J. M. (2005). Role of land-surface changes in Arctic summer warming. *science*, *310*(5748), 657-660.

Chipman, M. L., Clegg, B. F., & Hu, F. S. (2012). Variation in the moisture regime of northeastern interior Alaska and possible linkages to the Aleutian Low: inferences from a late-Holocene δ18O record. Journal of Paleolimnology, 48(1), 69-81.

Clegg, B. F., Kelly, R., Clarke, G. H., Walker, I. R., & Hu, F. S. (2011). Nonlinear response of summer temperature to Holocene insolation forcing in Alaska. Proceedings of the National Academy of Sciences, 108(48), 19299-19304.

Clegg, B. F., & Hu, F. S. (2010). An oxygen-isotope record of Holocene climate change in the south-central Brooks Range, Alaska. Quaternary Science Reviews, 29(7), 928-939.

Clegg, B. F., Clarke, G. H., Chipman, M. L., Chou, M., Walker, I. R., Tinner, W., & Hu, F. S. (2010). Six millennia of summer temperature variation based on midge analysis of lake sediments from Alaska. Quaternary Science Reviews, 29(23), 3308-3316.

Craig, H. (1961). Isotopic variations in meteoric waters. Science, (133), 1702-3.

Craig, H. (1965). The measurement of oxygen isotope paleotemperatures. In*Stable isotopes in oceanographic studies and paleotemperatures* (Vol. 3, p. 23). Lab. Geol. Nucl Pisa.

Dansgaard, W. (1964). Stable isotopes in precipitation. Tellus, 16(4), 436-468.

Eakins, J. A., & Morrison, R. T. (1978). A new procedure for the determination of lead-210 in lake and marine sediments. The International Journal of Applied Radiation and Isotopes, 29(9), 531-536.

Edwards, M. E., Bigelow, N. H., Finney, B. P., & Eisner, W. R. (2000). Records of aquatic pollen and sediment properties as indicators of late-Quaternary Alaskan lake levels. *Journal of Paleolimnology*, *24*(1), 55-68.

Ellis, J. M., & Calkin, P. E. (1984). Chronology of Holocene glaciation, central Brooks range, Alaska. Geological Society of America Bulletin, 95(8), 897-912.

Environmental Data Center Team. 2015. Meteorological monitoring program at Toolik, Alaska. Toolik Field Station, Institute of Arctic Biology, University of Alaska Fairbanks, Fairbanks, AK 99775. http://toolik.alaska.edu/edc/abiotic_monitoring/data_query.php

Epstein, S., Buchsbaum, R., Lowenstam, H. A., & Urey, H. C. (1953). Revised carbonate-water isotopic temperature scale. *Geological Society of America Bulletin*, *64*(11), 1315-1326.

Evison, L. H., Calkin, P. E., & Ellis, J. M. (1996). Late-Holocene glaciation and twentieth-century retreat, northeastern Brooks Range, Alaska. The Holocene, 6(1), 17-24.

Finkenbinder, M. S., Abbott, M. B., Edwards, M. E., Langdon, C. T., Steinman, B. A., & Finney, B. P. (2014). A 31,000 year record of paleoenvironmental and lake-level change from Harding Lake, Alaska, USA. *Quaternary Science Reviews*, *87*, 98-113.

Finney, B. P., Bigelow, N. H., Barber, V. A., & Edwards, M. E. (2012). Holocene climate change and carbon cycling in a groundwater-fed, boreal forest lake: Dune Lake, Alaska. *Journal of Paleolimnology*, *48*(1), 43-54.

Fleitmann, D., Burns, S. J., Mudelsee, M., Neff, U., Kramers, J., Mangini, A., & Matter, A. (2003). Holocene forcing of the Indian monsoon recorded in a stalagmite from southern Oman. *Science*, *300*(5626), 1737-1739.

Fritz, P., & Poplawski, S. (1974). 18 O and 13 C in the shells of freshwater molluscs and their environments. Earth and Planetary Science Letters, 24(1), 91-98.

Gaglioti, B. V., Mann, D. H., Jones, B. M., Pohlman, J. W., Kunz, M. L., & Wooller, M. J. (2014). Radiocarbon age-offsets in an arctic lake reveal the long-term response of permafrost carbon to climate change. *Journal of Geophysical Research: Biogeosciences*, *119*(8), 1630-1651.

Gupta, A. K., Anderson, D. M., & Overpeck, J. T. (2003). Abrupt changes in the Asian southwest monsoon during the Holocene and their links to the North Atlantic Ocean. *Nature*, *421*(6921), 354-357.

Higuera, P. E., Brubaker, L. B., Anderson, P. M., Hu, F. S., & Brown, T. A. (2009). Vegetation mediated the impacts of postglacial climate change on fire regimes in the south-central Brooks Range, Alaska. Ecological Monographs, 79(2), 201-219.

Hodell, D. A., Brenner, M., Curtis, J. H., & Guilderson, T. (2001). Solar forcing of drought frequency in the Maya lowlands. *Science*, *292*(5520), 1367-1370.

Hopkins, D. M., MacNeil, F. S., & Leopold, E. B. (1960). The coastal plain at Nome, Alaska: a late Cenozoic type section for the Bering Strait region. In *21st International Geologic Congress, Copenhagen, Part* (Vol. 4, pp. 46-57).

Hu, F. S., Ito, E., Brubaker, L. B., & Anderson, P. M. (1998). Ostracode geochemical record of Holocene climatic change and implications for vegetational response in the northwestern Alaska Range. *Quaternary Research*,*49*(1), 86-95.

Hu, F. S., Kaufman, D., Yoneji, S., Nelson, D., Shemesh, A., Huang, Y., ... & Brown, T. (2003). Cyclic variation and solar forcing of Holocene climate in the Alaskan subarctic. Science, 301(5641), 1890-1893.

Huybers, P. (2006). Early Pleistocene glacial cycles and the integrated summer insolation forcing. *Science*, *313*(5786), 508-511.

Intergovernmental Panel on Climate Change (Ed.). (2014). Climate Change 2013: The Physical Science Basis: Working Group I Contribution to the Fifth Assessment Report of the Intergovernmental Panel on Climate Change. Cambridge University Press.

IAEA/WMO (2014). Global Network of Isotopes in Precipitation. The GNIP Database. http://www.iaea.org/water.

Ito, E. (2001). Application Of Stable Isotope Techniques to Inorganic And Biogenic Carbonates. In Tracking environmental change using lake sediments (pp. 351-371). Springer Netherlands.

Kaufman, D. S., Ager, T. A., Anderson, N. J., Anderson, P. M., Andrews, J. T., Bartlein, P. J., ... & Wolfe, B. B. (2004). Holocene thermal maximum in the western Arctic (0–180 W). Quaternary Science Reviews, 23(5), 529-560.

Leng, M. J., & Marshall, J. D. (2004). Palaeoclimate interpretation of stable isotope data from lake sediment archives. Quaternary Science Reviews, 23(7), 811-831.

Leng, M. J., Lamb, A. L., Heaton, T. H., Marchall, J. D., Wolfe, B. B., Jones, M. D., ... & Arrowsmith, C. (2006). Isotopes in lake sediments (pp. 147-184). Springer Netherlands.

L'Heureux, M. L., Mann, M. E., Cook, B. I., Gleason, B. E., & Vose, R. S. (2004). Atmospheric circulation influences on seasonal precipitation patterns in Alaska during the latter 20th century. Journal of Geophysical Research: Atmospheres (1984–2012), 109(D6).

Mann, D. H., Groves, P., Reanier, R. E., & Kunz, M. L. (2010). Floodplains, permafrost, cottonwood trees, and peat: What happened the last time climate warmed suddenly in arctic Alaska?. *Quaternary Science Reviews, 29*(27), 3812-3830.

Mann, D. H., Peteet, D. M., Reanier, R. E., & Kunz, M. L. (2002). Responses of an arctic landscape to Lateglacial and early Holocene climatic changes: the importance of moisture. Quaternary Science Reviews, 21(8), 997-1021.

McCrea, J. M. (1950). On the isotopic chemistry of carbonates and a paleotemperature scale. *The Journal of Chemical Physics*, *18*(6), 849-857.

Oldfield, F., Appleby, P. G., & Battarbee, R. W. (1978). Alternative 210Pb dating: results from the New Guinea highlands and lough Erne.

Oswald, W. W., Anderson, P. M., Brown, T. A., Brubaker, L. B., Hu, F. S., Lozhkin, A. V., ... & Kaltenrieder, P. (2005). Effects of sample mass and macrofossil type on radiocarbon dating of arctic and boreal lake sediments. The Holocene, 15(5), 758-767.

Oswald, W. W., Brubaker, L. B., & Anderson, P. M. (1999). Late Quaternary vegetational history of the Howard Pass area, northwestern Alaska. *Canadian Journal of Botany*, *77*(4), 570-581.

Oswald, W. W., Brubaker, L. B., Hu, F. S., & Kling, G. W. (2003). Holocene pollen records from the central Arctic Foothills, northern Alaska: testing the role of substrate in the response of tundra to climate change. Journal of Ecology, 91(6), 1034-1048.

Oswald, W. W., Gavin, D. G., Anderson, P. M., Brubaker, L. B., & Hu, F. S. (2012). A 14,500-year record of landscape change from Okpilak Lake, northeastern Brooks Range, northern Alaska. Journal of Paleolimnology, 48(1), 101-113.

Prowse, T. D., Wrona, F. J., Reist, J. D., Gibson, J. J., Hobbie, J. E., Lévesque, L. M., & Vincent, W. F. (2006). Climate change effects on hydroecology of Arctic freshwater ecosystems. *AMBIO: A Journal of the Human Environment*, *35*(7), 347-358.

Reimer, P. J., Baillie, M. G., Bard, E., Bayliss, A., Beck, J. W., Blackwell, P. G., ... & Weyhenmeyer, C. E. (2009). IntCal09 and Marine09 radiocarbon age calibration curves, 0-50,000 years cal BP.

Rodionov, S. N., Bond, N. A., & Overland, J. E. (2007). The Aleutian Low, storm tracks, and winter climate variability in the Bering Sea. *Deep Sea Research Part II: Topical Studies in Oceanography*, *54*(23), 2560-2577.

Röthlisberger, F., & Geyh, M. A. (1986). 10000 Jahre Gletschergeschichte der Erde: Teil I: e. Vgl. zwischen Nord-u. Südhemisphäre; Alpen-Skandinavien-Himalaya-Alaska-Südamerika-Neuseeland. Teil 2: mit e. Beitr. 14C-Daten zu Gletscherständen-Probleme der Deutung. Sauerländer.

Solomina, O. N., Bradley, R. S., Hodgson, D. A., Ivy-Ochs, S., Jomelli, V., Mackintosh, A. N., ... & Young, N. E. (2015). Holocene glacier fluctuations. Quaternary Science Reviews, 111, 9-34.

Solomina, O., & Calkin, P. E. (2003). Lichenometry as applied to moraines in Alaska, USA, and Kamchatka, Russia. *Journal Information*, *35*(2).

Soon, W. W. H. (2005). Variable solar irradiance as a plausible agent for multidecadal variations in the Arctic-wide surface air temperature record of the past 130 years. *Geophysical Research Letters*, *32*(16).

Stafford, J. M., Wendler, G., & Curtis, J. (2000). Temperature and precipitation of Alaska: 50 year trend analysis. Theoretical and Applied Climatology, 67(1-2), 33-44.

Steinhilber, F., Abreu, J. A., Beer, J., Brunner, I., Christl, M., Fischer, H., ... & Wilhelms, F. (2012). 9,400 years of cosmic radiation and solar activity from ice cores and tree rings. Proceedings of the National Academy of Sciences, 109(16), 5967-5971.

Stone, R. S., Dutton, E. G., Harris, J. M., & Longenecker, D. (2002). Earlier spring snowmelt in northern Alaska as an indicator of climate change. Journal of Geophysical Research: Atmospheres (1984–2012), 107(D10), ACL-10.

Stuiver M, Reimer PJ (1993) Extended 14C database and revised CALIB radiocarbon calibration program. Radiocarbon, 35:215–230.

Urey, H. C., Lowenstam, H. A., Epstein, S., & McKinney, C. R. (1951). Measurement of paleotemperatures and temperatures of the Upper Cretaceous of England, Denmark, and the southeastern United States. *Geological Society of America Bulletin*, *62*(4), 399-416.

Wiles, G. C., Jacoby, G. C., Davi, N. K., & McAllister, R. P. (2002). Late Holocene glacier fluctuations in the Wrangell Mountains, Alaska. Geological Society of America Bulletin, 114(7), 896-908.

Young, N. E., Briner, J. P., & Kaufman, D. S. (2009). Late Pleistocene and Holocene glaciation of the Fish Lake valley, northeastern Alaska Range, Alaska. Journal of Quaternary Science, 24(7), 677-689.

Zhang, T., Osterkamp, T. E., & Stamnes, K. (1996). Some characteristics of the climate in northern Alaska, USA. Arctic and Alpine Research, 509-518.